Polymer Degradation and Stability

Effect of an organoclay on the photochemical transformations of a PBAT/PLA blend and morpho-chemical features of crosslinked networks

--Manuscript Draft--

Manuscript Number:	PDST-D-21-00101
Article Type:	Research Paper
Section/Category:	Green Flame Retardants, Nanocomposites, Thin Coating, Textiles
Keywords:	photo-oxidation; crosslinking; nanocomposites; bioplastic; Cloisite; PBAT; PLA.
Corresponding Author:	Roberto Scaffaro, Prof. University of Palermo Palermo, ITALY
First Author:	Roberto Scaffaro, Prof.
Order of Authors:	Roberto Scaffaro, Prof.
	Andrea Maio
	Michele Gammino
	Francesco Paolo La Mantia
Abstract:	In this work, we report the effect of an organoclay on the photochemical weathering of nanocomposites based on a poly(butylene adipate-co-terephthalate) (PBAT) /poly(lactic acid) (PLA) blend. The evolution of physicochemical properties was monitored by integrating several techniques. The results demonstrated the pro-degradant role of nanofiller, which promoted both scission and crosslinking photochemical reactions, with the former being dominant at the early stages of photo-oxidation, and the latter prevailing after long-term exposure. A robust relationship was found between the molecular transformations of the polymer macromolecules and the morpho-mechanical properties of irradiated films. Moreover, the analysis of insoluble fractions extracted from nanocomposites pointed out that free-standing, porous structures, displaying an unprecedented thickness as great as 100 μm, were formed, thus unambiguously demonstrating that the organoclay increased the propagation depth of photochemical crosslinking reactions by 10 times with respect to previously reported results on PBAT. The pore architecture and chemical structure of such crosslinked networks proved to change depending on organoclay content of films.
Suggested Reviewers:	Sahar Al-Malaika s.al-malaika@aston.ac.uk
	Sabu Thomas sabuthomas@mgu.ac.in

Dear Editor,

We are pleased to submit our manuscript entitled: “Effect of an organoclay on the photochemical transformations of a PBAT/PLA blend and morpho-chemical features of crosslinked networks”.

This work is focused on the study of photochemical transformations occurring on a commercial blend based on poly(butylene adipate-co-terephthalate) (PBAT) and poly(lactic acid) (PLA), in the presence of an organoclay. The materials underwent accelerated weathering at 70 °C under UV-exposure and the time-dependent evolution of physicochemical properties was monitored, aiming at providing a robust relationship between photo-induced structural changes and macroscopic properties. The degradation of materials, at the early stage of exposure, was mainly governed by Norrish I and II scission reactions, while crosslinking events involving PBAT radicals became the prevalent mechanism in long-term irradiated samples.

Nanoclay, owing to the presence of iron ions and alkylammonium salts, exerted a remarkable pro-degradant effect, thus increasing not only the kinetics but even the propagation depth of all the photolytic reactions. In this latter regard, the analysis of insoluble fractions extracted from nanocomposites pointed out that free-standing structures with interconnected pores were formed, displaying an unprecedented thickness as great as 100 μm, i.e., 10 times higher than the values typically reported for the propagation of photodegradation pathways in PBAT films. What is more, the pore architecture and chemical structure of such crosslinked networks proved to change depending on organoclay content of films.

The outcomes of this research, beyond the in-depth understanding of photochemical aging of PBAT/PLA blends in the presence of an organoclay, might even pave the road for the future development of porous structures from bioplastic wastes. In this context, giving the fact that photochemical weathering is well-known to dramatically affect the biodegradability of PBAT-based materials, the possibility to reuse them to fabricate high-added value porous materials may partially mitigate their overall environmental impact, in full compliance with circular economy and zero-waste concepts.

Therefore, owing to the novelty and the relevance of results, which encompass both chemical and engineering aspects of polymer degradation, we hope that the paper can be suitable for being published on Polymer Degradation and Stability.

Sincerely yours,

Roberto Scaffaro

Andrea Maio

Michele Gammino

Francesco Paolo La Mantia

- Thick films made of PBAT, PLA and nanoclay were UV-irradiated for 120 hours.
- Photodegradation of PBAT/PLA blend involved scission and crosslinking events.
- Clay increased propagation depth of photochemical pathways by 10 times.
- Freestanding, well-organized structures with interconnected pores were isolated.
- Clay content influenced morpho-chemical features of crosslinked networks.

Effect of an organoclay on the photochemical transformations of a PBAT/PLA blend and morpho-chemical features of crosslinked networks

Roberto Scaffaro, Andrea Maio, Michele Gammino, Francesco Paolo La Mantia

Department of Engineering, University of Palermo, Viale delle Scienze, ed. 6, 90128 Palermo, Italy

Abstract

In this work, we report the effect of an organoclay on the photochemical weathering of nanocomposites based on a poly(butylene adipate-co-terephthalate) (PBAT)/poly(lactic acid) (PLA) blend.

The evolution of physicochemical properties was monitored by integrating several techniques. The results demonstrated the pro-degradant role of nanofiller, which promoted both scission and crosslinking photochemical reactions, with the former being dominant at the early stages of photo-oxidation, and the latter prevailing after long-term exposure. A robust relationship was found between the molecular transformations of the polymer macromolecules and the morpho-mechanical properties of irradiated films.

Moreover, the analysis of insoluble fractions extracted from nanocomposites pointed out that free-standing, porous structures, displaying an unprecedented thickness as great as 100 μm, were formed, thus unambiguously demonstrating that the organoclay increased the propagation depth of photochemical crosslinking reactions by 10 times with respect to previously reported results on PBAT. The pore architecture and chemical structure of such crosslinked networks proved to change depending on organoclay content of films.

Keywords: photo-oxidation; crosslinking; nanocomposites; bioplastic; Cloisite; PBAT; PLA.

1. Introduction

The evolution of bioplastics related research has recently changed directions and guidelines, with the latest generation of green materials moving toward the development of durable bioplastics[1]. The goal is to conjugate the low environmental impact of bioplastics, made by renewable carbon sources, with the achievement of good mechanical performance and durability, so as to render these materials desired for long-term applications in automotive, electronics and other fields[1,2]. Therefore, the ultimate challenge is to achieve bioplastics that are capable of resisting against UV, heat, and mechanical solicitations during their lifetime, while offering the possibility to be disintegrated in *ad hoc* designed, appropriate conditions at their end-use [3].

Unfortunately, currently widespread bioplastics often show many drawbacks both in durability and controlled disintegrability, but even in terms of poor mechanical toughness and strength [1,3]. Performance limitations and high cost of such green polymers could be mitigated through the incorporation of nanofillers [4–6]. In this perspective, nanoclays, nanocarbons and even renewable nanoparticles, including nanocellulose or lignin, have been studied as promising fillers for bioplastic-based nanocomposites [7–13]. However, while the effect of such additives on the mechanical and thermomechanical properties of various bioplastics was abundantly studied, their effect on the durability of resulting materials have been only occasionally reported [9,13,14].

In the frame of this work, we examined the case of a commercial blend based on Poly(lactic acid) (PLA) and Poly(butylene adipate-co-terephthalate) (PBAT), which are considered among the most promising biodegradable polymers, reinforced with relatively small amounts of an organoclay (Cloisite 15A). In fact, although both PLA and PBAT belong to renewable and compostable poly-α-esters, their degradation under UV-exposure may be triggered in different ways and therefore follow different pathways [2,15,16]. Furthermore, the presence of metal ions and alkyl ammonium salts in such nanofillers is supposed to somehow affect the photochemical transformations of

PBAT/PLA blend, whose comprehension could be useful to provide further guidance on the development of durable bioplastic-based nanocomposites for outdoor applications.

2. Experimental section

2.1 Materials

A commercial PBAT/PLA blend (trade name: Ecovio F23B1, BASF, Germany), consisting of 84% PBAT, 4% of PLA, and 12% of inert particles/additives was selected as a matrix [17]. According to technical datasheet, it is fully compostable and displays density of 1.25 g/cm^3 and MFI about equal to 10 g/10 min (at 190°C and 5 Kg).

The nanofiller adopted in this study is a sample of Cloisite 15A (CL15A), i.e., a montmorillonite modified with alkyl ammonium salts, produced by Southern Clay Product. The organic modifier consists of two methyl groups and two organophilic tails (HT). The amount of organic modifier (MER) used is 95 meq/100g.

Prior to processing, all the materials underwent vacuum-drying at T=70 °C for 4 hours, aiming to prevent hydrolytic degradation of the polymers during processing.

2.2 Preparation of nanocomposites

The process adopted to fabricate nanocomposite sheets is schematized in **Figure 1**.

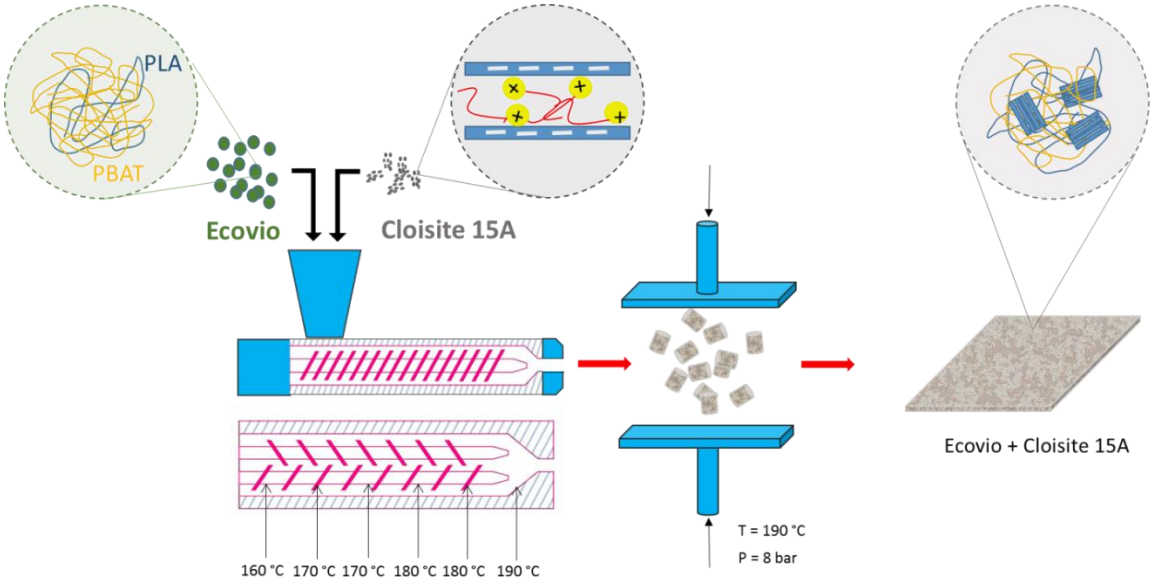

Figure 1. Fabrication route to obtain nanocomposites.

More in detail, nanocomposites containing either 2 or 5 wt.% CL15A, respectively indicated as C-2 and C-5, were prepared by using a twin-screw extruder. Thermal extrusion profile chosen was (from feeding to die): 160-170-170-180-180-190 °C. The material coming from extruder was then processed into 300 μm thick films by compression molding (T=190 °C, p=8 bar), by using a laboratory press (Carver, USA).

2.3 Photodegradation tests

The films obtained have been subjected to accelerated weathering at 70 °C in Q-UV chamber (QLabs Corp., USA) equipped with eight UVB-313 lamps by irradiating the samples respectively for 6, 12, 24, 48, 120 h.

2.4 Characterizations

Pristine and photo-oxidized films, as well as their corresponding gel fractions, were characterized from a morphological, chemical, physical, and mechanical point of view. Morphology has been investigated by scanning electron microscopy (SEM) imaging, carried out with a Phenom Pro X instrument (Thermo Fisher Scientific, Waltham, MA, USA).

Mechanical properties of the samples were evaluated by tensile tests, performed by means of an Instron 3365 (Instron, Norwood, MA, USA) dynamometer, by imposing an initial crosshead speed of 1 mm/min (until 3 min), and a second crosshead speed increased to 100 mm/min, up to specimen failure, according to ISO 527-3 standard. At least 10 replicates for each experimental run were tested and the salient data, i.e.: elastic modulus (E), tensile strength (TS) and elongation at break (EB), were provided as mean values and standard deviations.

Melt flow index (MFI) measurements were conducted at 190°C and 5 Kg by means of a CEAST (Italy) equipment.

Photo-degraded samples were then extracted in a Soxhlet apparatus using boiling chloroform, aiming to analyze the gel fraction formed.

In order to consider solely the gel formed due to photolysis, apart from the contribution of eventual mineral residue of clay and other additives trapped in the filter and of PBAT crosslinked during processing, photo-triggered gel fraction ($Gel_{p-t}\%$) was assessed by equation (1):

$$Gel_{p-t}\% = \frac{W_{gel}(t) - W_{gel,0}}{W_{gel,0}} 100 \qquad (1)$$

Where $W_{gel}(t)$ and $W_{gel,0}$ respectively indicate the gel amounts at a given exposure time and at t=0.

Photochemical transformations of the materials were analyzed by Fourier-transform infrared (FTIR) spectroscopy in attenuated total reflection (ATR) mode, using a FT-IR/NIR Spectrum 400 spectrophotometer (Perkin-Elmer, Waltham, MA, USA). Spectra were obtained in the 4000–400 cm^{-1} wavenumber range, by collecting 32 scans with resolution equal to 4 cm^{-1}. Investigations were performed onto both films and gel fraction extracted. When needed, spectra were deconvoluted by multi-peak fitting analysis (Origin Lab 9.0 software).

It was evaluated the irradiation time-dependent evolution of spectral features of particular interest, including the characteristic bands of PBAT and PLA and those attributable to emerging functional

groups, including hydroxyl, methyl, aldehyde and various tri-substituted benzenes and benzophenone-like structures.

3. Results and discussion

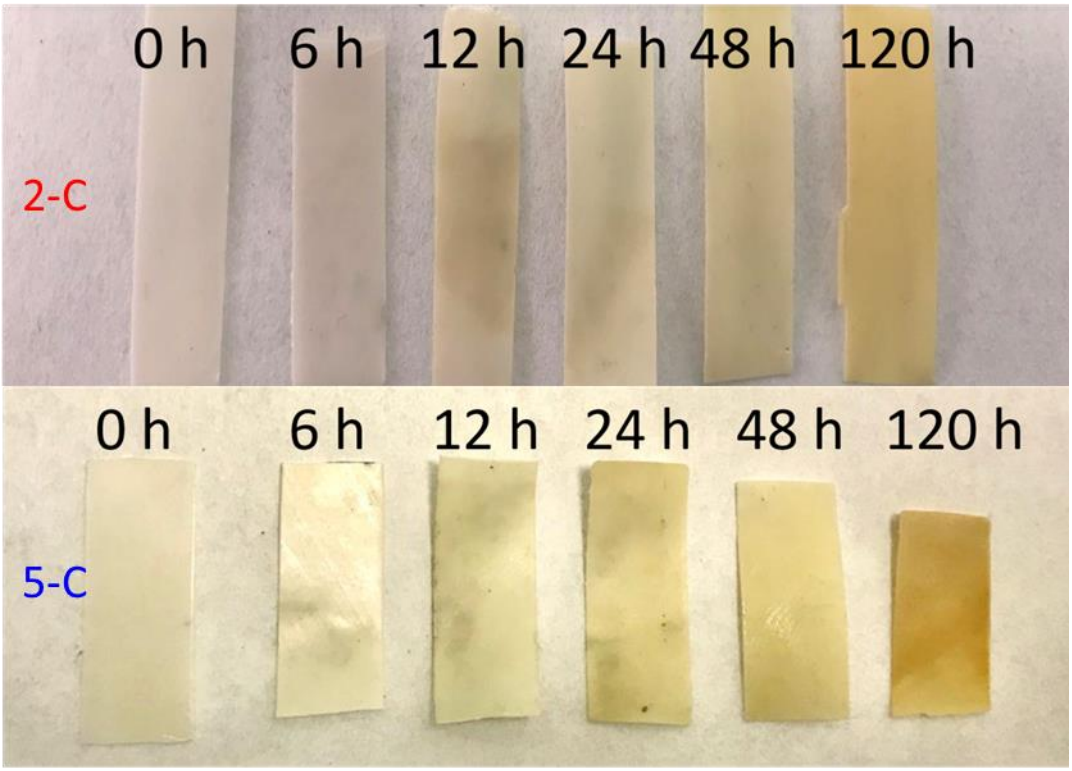

Figure 2. Visual analysis of macroscopic changes occurred during photo-oxidation: digital photographs of the surface of irradiated samples.

Figure 2 provides the digital photographs of the surfaces exposed to UV-irradiation of 2-C and 5-C films. The impact of photochemical degradation on the appearance and physical properties of samples appeared quite clear yet at a macroscale level, with all the irradiated specimens showing a progressive yellowing that became particularly evident in long-term photolyzed films, reasonably due to the formation of chromophore compounds.

Beyond this, the typical flexibility of such materials proved to be gradually suppressed with outstanding embrittlement. Hence, the irradiation time-dependent evolution of mechanical

properties was monitored, and the salient results obtained by tensile tests, in terms of elongation at break (EB), and elastic modulus (E) are respectively provided in **Figure 3 a-b**.

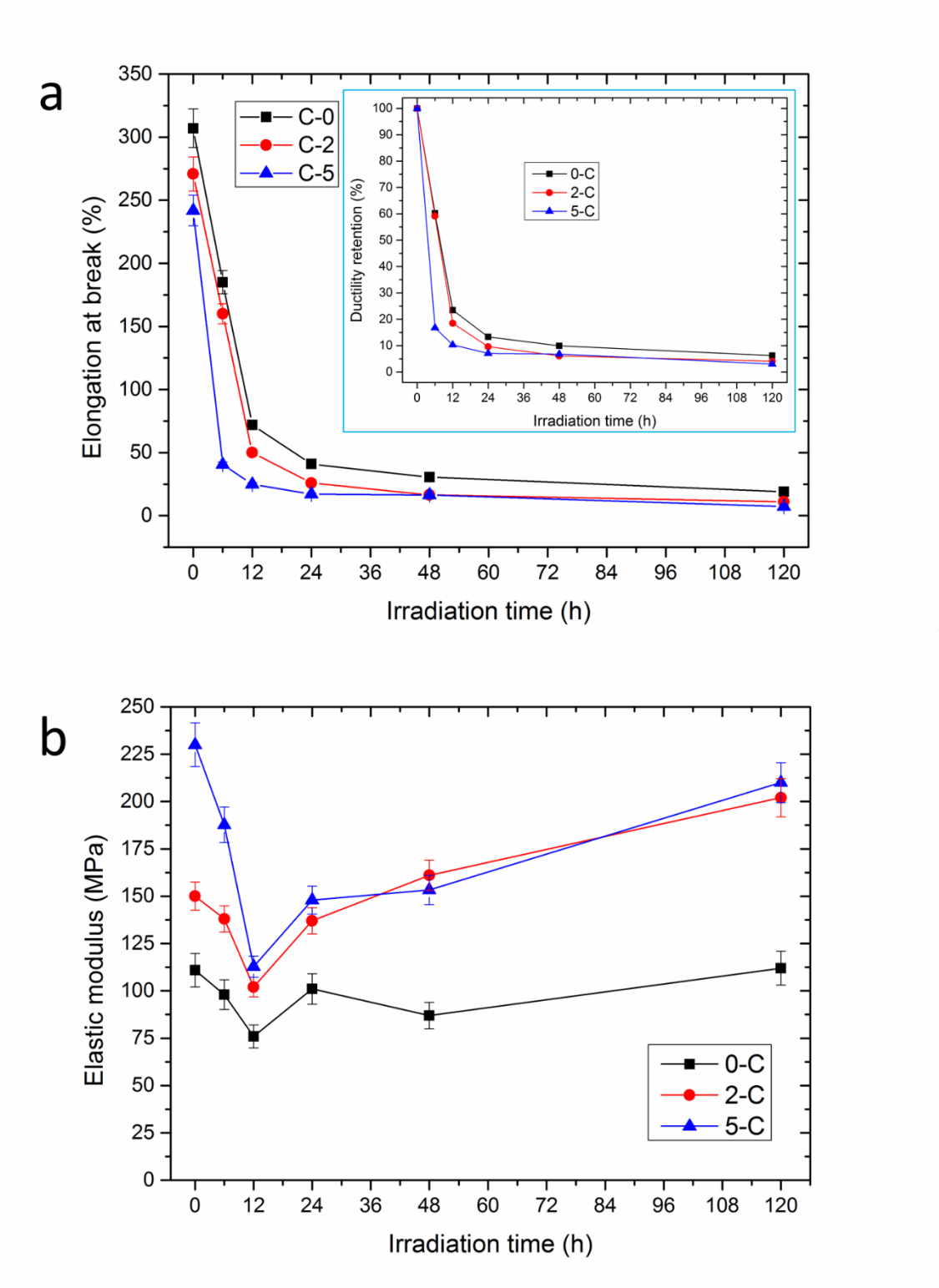

Figure 3. Evolution of elongation at break (a) and elastic modulus (b) as a function of irradiation time. Inset of panel (a) provides the retention of the initial ductility for all the samples.

Although the dimensionless elongation at break of all the samples proved to decrease as a function of irradiation time, such reduction was found to be more dramatic and rapid for nanocomposites, especially at high clay content. In fact, while 0-C and 2-C films irradiated for 6 h retained 60% of their initial deformability, ductility retention of 5-C series materials in the same conditions was only 17%. It is worth mentioning that clay content affected such decay until 48 h exposure, while long-term irradiated nanocomposites displayed practically the same values of ductility retention, regardless of filler concentration.

As regards elastic modulus (Fig. 3b), the effect of formulation on unirradiated samples is quite significant. In fact, at t=0, stiffness of nanocomposites proved to monotonically increase with filler content, going from 110 MPa for neat polymer up to 230 MPa (for 5-C). This is expectedly due to the stiffness contrast between matrix and filler and intercalation/exfoliation phenomena, abundantly reported in literature [18–21].

However, despite their starting differences, all the materials experienced an initial decrease of elastic modulus as a function of irradiation time until 12 hours. Thereafter, a progressive increase of this property was observed for nanocomposite systems and, at the end of experiment (t=120 hours) 2-C showed elastic modulus even higher than that exhibited before irradiation. The apparently strange behavior of such curves might be due to the concomitance of several phenomena with opposite repercussions on this property. In fact, Ecovio is a blend of two polymers that follow different photochemical transformations, when exposed to UV-light. More in detail, PLA phase is known to undergo Norrish II scission events with a progressive shortening of polymer chains that may provoke a decay of elastic modulus [2]. On the other hand, in a semi-crystalline polymer as PLA, the shorter the chains, the higher their ability to crystallize with obvious stiffening and embrittlement [22,23]. Regarding PBAT phase, instead, UV exposure is known to cause

simultaneous cross-linking and cleavage of PBAT chains, thus leading to the formation of both an insoluble polyester network and low molar mass PBAT chain fragments [24–26].

The outcomes of mechanical tests were corroborated with MFI and spectroscopic analysis, aiming to provide a deeper comprehension of the complex photochemical transformations occurred in such systems.

MFI values as a function of irradiation time are reported in **Figure 4**.

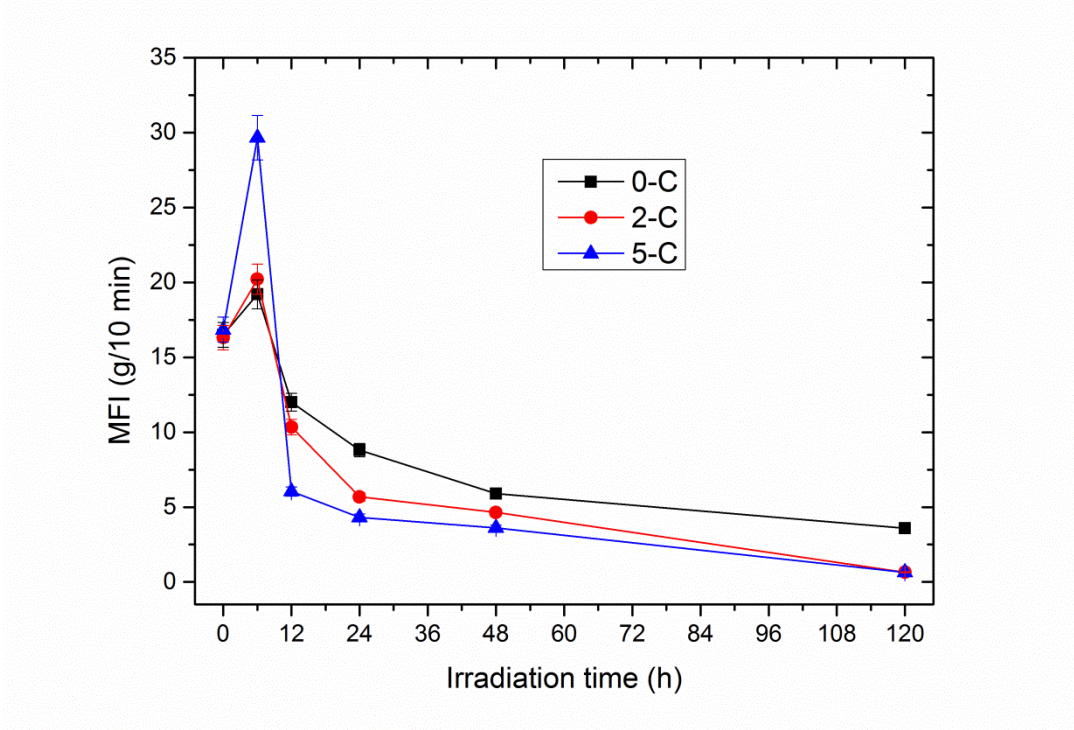

Figure 4. Melt Flow Index of 0-C, 2-C and 5-C, plotted as a function of irradiation time.

Expectedly, and in full agreement with mechanical results, MFI follows the opposite trend as that of elastic modulus: at low irradiation times, namely at t=6 h, all the materials experienced an increase of fluidity, reasonably due to decay of molecular weight. After 12 hours exposure, MFI start decreasing, likely owing to the triggering of photo-crosslinking reactions which led to an increase of melt viscosity, up to reach a value as low as 0.46 and 0.65 g/10 min for the samples 2-C and 5-C irradiated for 120 hours, respectively. Notably, nanocomposites displayed more significant changes

when compared to 0-C. Moreover, the maximum intensity of 5-C proved to be higher than that of 2-C, with a drop occurring steadily and faster (at t=12 h) than 2-C, thus letting envisage that nanoclay content could have played a somehow significant role in both chain scission and crosslinking reactions kinetics.

The effect of UV-exposure on the morphology of the samples was assessed by SEM analysis. **Figure 5** provides SEM micrographs of the surfaces of 2-C (a-c) and 5-C films (d-f) untreated and irradiated at 12 h and 120 h.

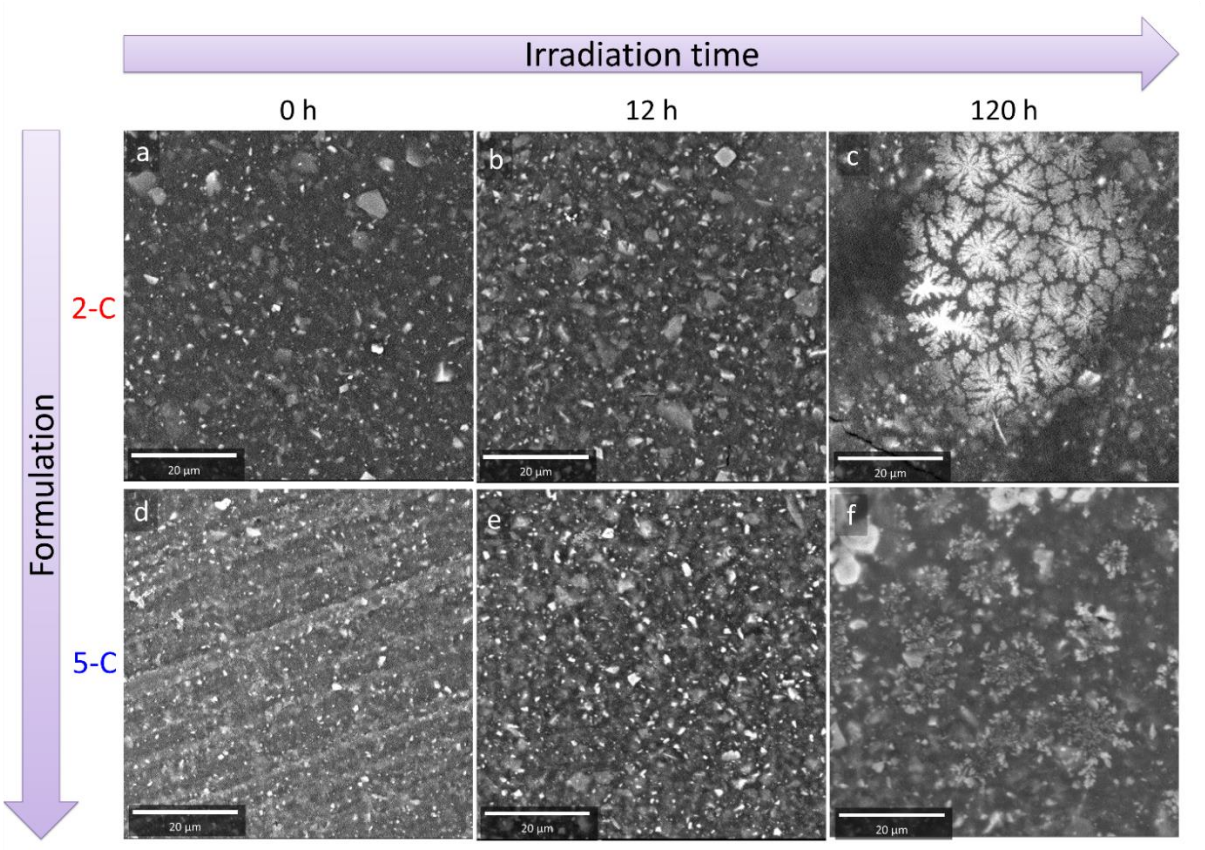

Figure 5. SEM micrographs of the exposed surfaces of 2-C (a-c) and 5-C (d-f) films irradiated at different times.

Moving from left to right panels it is possible to observe the evolution of surface morphology as a function of irradiation time, while the effect of nanoclay content for a given irradiation time can be assessed by moving from top to bottom panels. Both samples, prior to UV-exposure, display the typical features of composite systems, where it can be easily recognized a dispersed phase

consisting of micrometric particles (already present in the formulation of Ecovio) and submicrometric/nanometric fillers (reasonably clay). The samples irradiated for 12 hours substantially retain the same morphology, while the effect of irradiation time was particularly intense and evident in the samples UV-exposed for 120 h that displayed significant alterations, likely due to the formation of well-extended cross-linked networks. Notably, the surfaces of 2-C and 5-C photo-oxidized for 120 hours were even found to strongly differ each other.

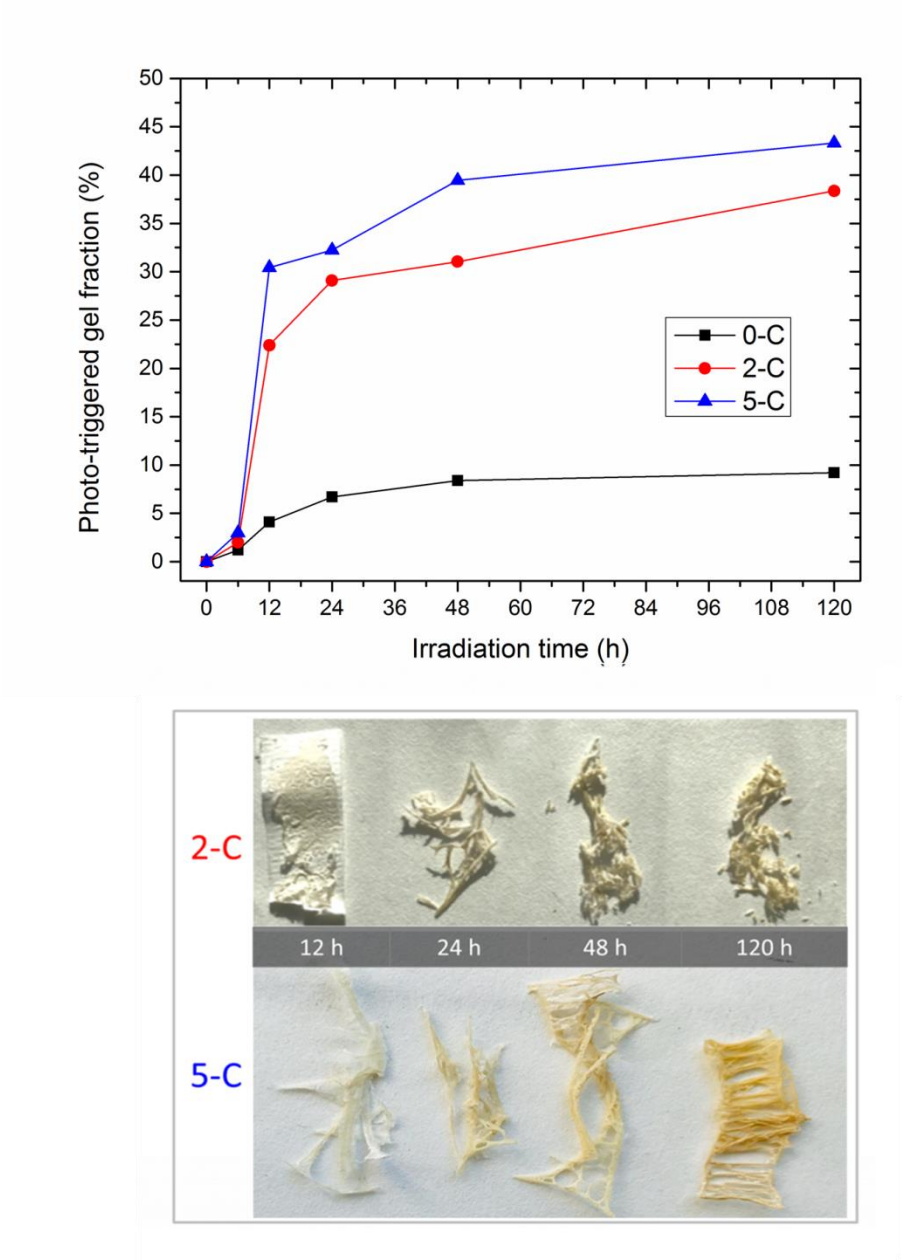

Figure 6. Photo-triggered gel fraction (%) as a function of irradiation time (top panel), together with digital photographs of gel fractions extracted from 2-C and 5-C irradiated at different times (bottom panel).

Hence, the eventual gel fraction formed due to photo-crosslinking reactions was extracted and analysed.

In **Figure 6**, photo-triggered gel fractions extracted from the irradiated samples are provided as a function of irradiation time, together with digital photographs of the structures formed. When compared to neat matrix, the nanocomposites display significantly larger amounts of insoluble fractions. Surprisingly, for the samples C-2 and C-5, after a certain extent of crosslinking reactions (t>12 h), it was even possible to isolate the insoluble aliquots, self-organized into freestanding structures, which appeared quite different in colour and morphology already at a macroscale level, in full agreement with the appearance of photodegraded films (see again Fig. 2).

SEM micrographs at different magnifications of the gel fractions extracted from 2-C (**Fig. 7**) and 5-C (**Fig. 8**) films irradiated for 120 h revealed the porous structure of both samples, and their different pore architecture. 2-C insoluble fraction (Fig. 7) displayed a thin, dense skin and a porous core with regular, spherical pores having diameters below 15 μm; 5-C (Fig. 8) showed a fibrous structure, bearing the presence of irregularly shaped, quite larger pores (20-30 μm), throughout all the sample. The morphological differences between the insoluble fractions of 2-C and 5-C are consistent with those observed in the surfaces of entire films (see again Fig. 5c and Fig. 5f) and suggest that the content of clay could have played a crucial role in both triggering and propagating crosslinking reactions.

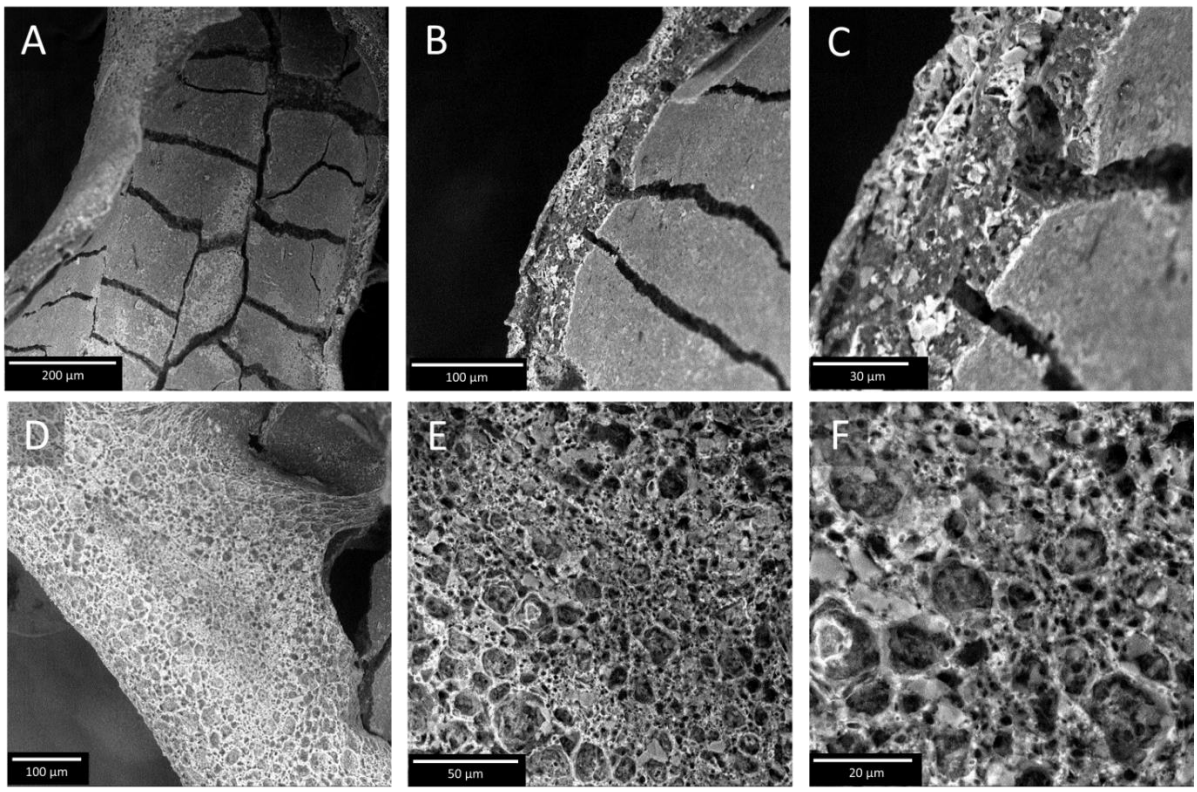

Figure 7. Surface (A-B) and cross-sectional (C-F) SEM micrographs at different magnifications of gel fraction extracted from 2-C films irradiated for 120 hours.

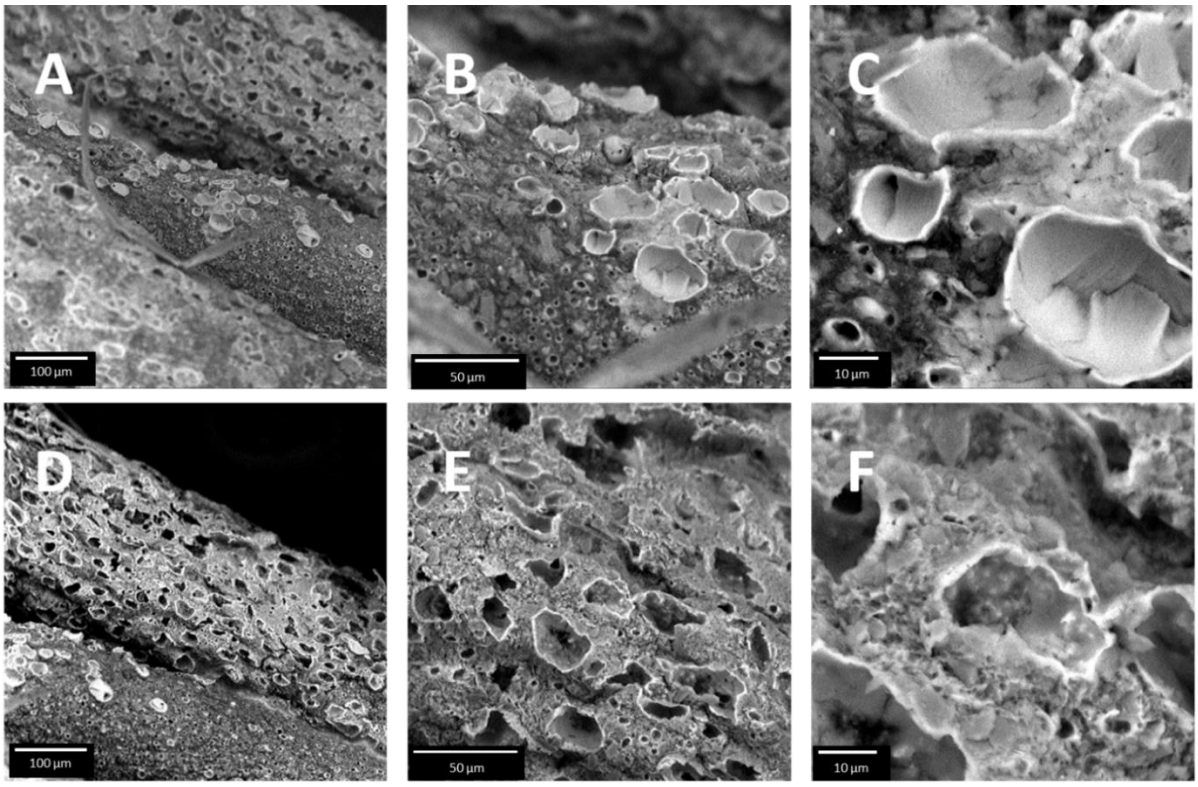

Figure 8. Top (a-c) and cross-sectional (d-f) SEM micrographs at different magnifications of gel fraction extracted from 5-C films irradiated for 120 hours.

Based on recently reported studies, the propagation of crosslinking reactions in the bulk of irradiated PBAT thin films did not exceed 10-11 μm [24,26]. The materials investigated in this work are much thicker (300 μm), hence the insoluble fraction was expected to be negligible. This is in full agreement with the experiments conducted on C-0, where the photo-triggered gel fraction formed during UV was found below 10% and it was not possible to isolate any freestanding network from the filter. Surprisingly, the presence of nanoclay dramatically increased not only gel content but also the thickness of insoluble networks, which exceeded 100 microns, thus indicating that photochemical crosslinking reactions propagated into the bulk.

A common way to monitor photochemical transformations occurring during UV-irradiation is FTIR analysis. Hence, FTIR in ATR mode was used to validate the mechanisms generally proposed for PBAT and PLA photo-degradation and to assess the eventual implications of integrating an organoclay into such matrix.

FTIR spectra collected for 5-C materials at the various photo-oxidation times are shown in **Figure 9**, with a special focus on four spectral regions: 3700-2700 cm^{-1} (panel a), 1900-1000 cm^{-1} (panel b), 1350-1000 cm^{-1} (panel c), and 780-700 cm^{-1} (panel d), useful for investigating the evolution of the main bands of interest, whose peak position and assignation are reported in **Table 1**. FTIR spectra collected for 2-C series are qualitatively similar and provided in Figure S1 (see SI).

Table 1. Characteristic FTIR modes of PBAT and PLA

FTIR mode	**Peak position (cm^{-1})**	
	PBAT	**PLA**
$-\boldsymbol{CH_2}-$ stretching	2957, 2874	2947
$-\boldsymbol{C=O}$ stretching	1715, 1731	1751

$-\boldsymbol{CH_3}$ bending	1453	1455
$-\boldsymbol{C-O}-$ stretching	1269, 1165	1268, 1184
	1120, 1104	1129, 1087
$-\boldsymbol{C-C}-$ stretching	-	956
$-\boldsymbol{CH}-$ bending	-	868, 755
$-\boldsymbol{CH_2}-$ rocking	729	-

In all the spectra it is possible to recognize the typical bands of PBAT, which is the main component of Ecovio blend, and those, less intense, of PLA [9,27]. However, all these signals proved to change their intensity as a function of exposure time. It was generally observed an initial increase of the bands corresponding to -OH vibrations at ca. 3400-3450 cm^{-1} (**Fig. 9a**) up to reach a maximum at 12 h irradiation time, followed by the progressive depletion of intensity for longer exposures. The carbonyl band of pristine films has three main contributions: a weak peak at 1750 cm^{-1}, ascribed to –C=O stretching of PLA, a sharp peak centered at 1730 cm^{-1} with a shoulder located at 1715 cm^{-1}, which are associated to –C=O stretching of PBAT. Upon increasing irradiation time, it was observed the progressive depletion of signals due to carbonyls of PBAT, while those associated to PLA displayed intensities higher than that of untreated material, with a maximum observed at 12 h.

Even the intensity of the bands ascribed to C-H stretching vibrations of -CH groups (2950-2850 cm^{-1}) and to C=C symmetric stretching (1650 cm^{-1}) displayed a similar behavior, with a maximum at 12 h. These features suggest that, within this investigation time, the material underwent at least two competing photochemical transformations, with the former one, predominant at early stages of photo-oxidation, generating -OH moieties and C=C bonds, but also aldehydes, which were then consumed by the triggering/prevailing of the latter mechanism at times longer than 12 hours. Both photochemical reactions provoked the generation of carboxyl moieties in PLA, likely due to

cleavage of ester bonds, accompanied by the consumption of carbonyl groups of PBAT, unambiguously confirmed by the progressive and simultaneous depletion of both C=O and C-O signals, respectively centered at 1720 cm^{-1} and 1275-1250 cm^{-1}, which were presumably involved in crosslinking reactions [9].

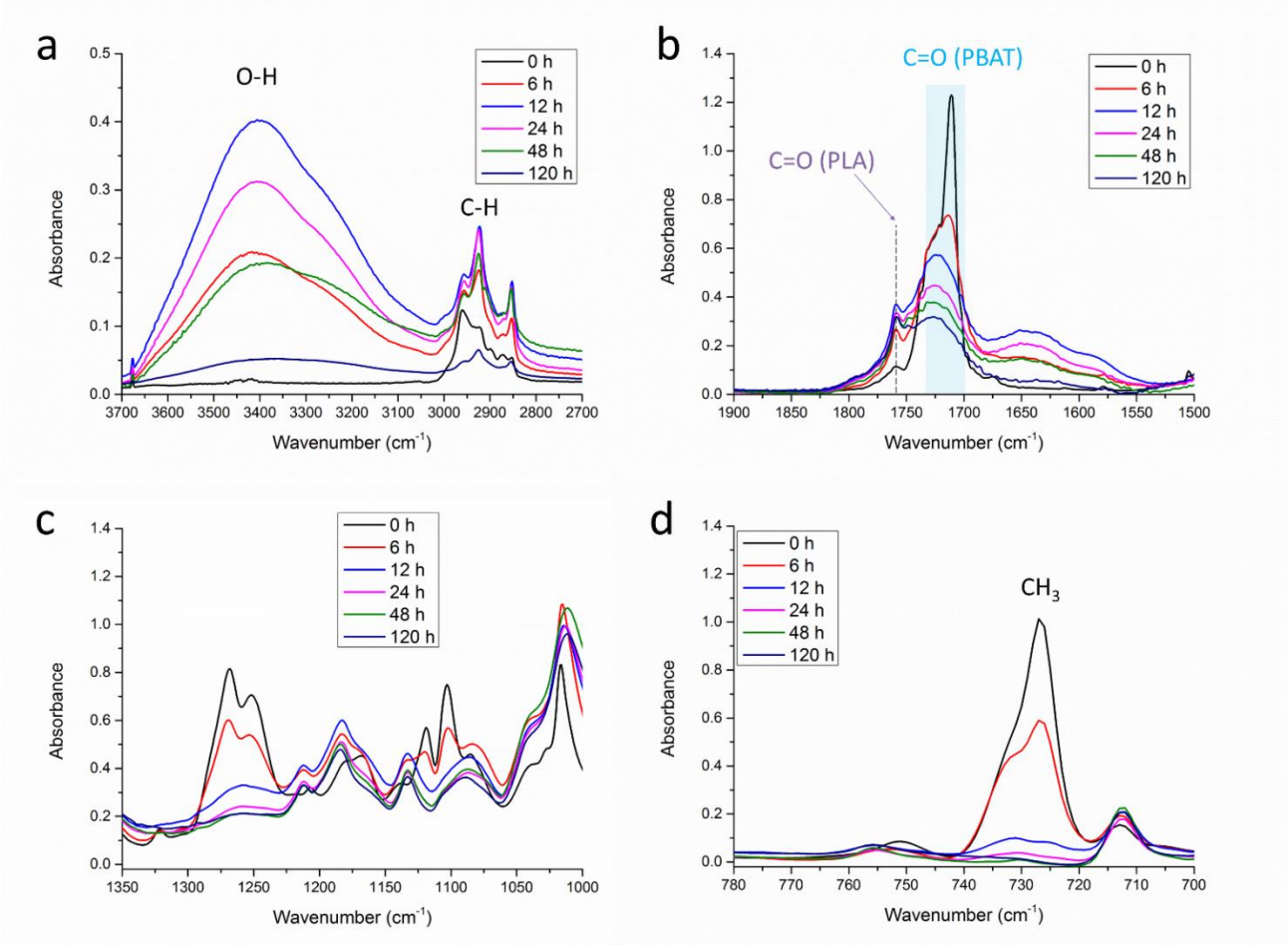

Figure 9. FTIR/ATR spectra of 5-C at different irradiation times: 3700-2700 cm^{-1} (a), 1900-1000 cm^{-1} (b), 1350-1000 cm^{-1} (c), and 780-700 cm^{-1} (d).

Based on the data collected and the previous studies reported on similar systems, the degradative phenomena occurring in PBAT, PLA and organoclay have been hypothesized and provided in **Figure 10**. The degradation of PBAT and PLA, at least in the first 12 hours, follows the typical Norrish I and II reaction pathways, according to the scientific literature. The former leads to the

formation of hydroxyl- and aldehyde-terminated chains, whereas $-CH=CH_2$ and $-COOH$ species could be originated by PLA degradation via Norrish II mechanism.

Of course, as the concentration of degradation products increases, the recombination between radical species originating from PLA and PBAT chain cleavage may occur, with ensuing formation of branched and crosslinked structures. In particular, it was unambiguously detected that various trisubstituted benzophenones and benzenes are responsible for crosslinking of irradiated PBAT, which occurs via a radical mechanism involving either acyl or phenyl radicals (see again crosslinking events in **Fig. 10**) [24–26]. It was also well-established that benzophenone moieties, acting as photosensitizers, tend to accelerate photochemical transformation during long-term UV exposure of materials containing PBAT [24–26]. With respect to existing literature, in this case we should consider the role exerted by organoclay in propagating such reactions into the bulk. In fact, alkylammonium salts of Cloisite 15A are known to thermally decompose already during melt processing, via Hoffman elimination and subsequent nucleophilic substitution (SN_2) reactions.

During degradation, alkylammonium cation loses an amine group and an α-olefin, resulting in the formation of different chromophore compounds, such as carboxylic and aldehyde groups, leaving an acidic proton on the surface of the clay [19]. The presence of such acidic sites catalyzes the degradation of both organic modifier and polymer matrix, thus accelerating the processes described above and somehow exerting a crucial role on the extent of degradation [19]. Moreover, also structural Fe (II) ions naturally contained in the clays demonstrated a strong photocatalytic activity, ascribed to their oxidation to hydrous ferric oxide, especially in the presence of organic compounds [28].

In fact, data obtained from mechanical, rheological, spectroscopic, and morphological analyses outline a strong relationship between formulation, namely nanoclay content, and extent of degradation.

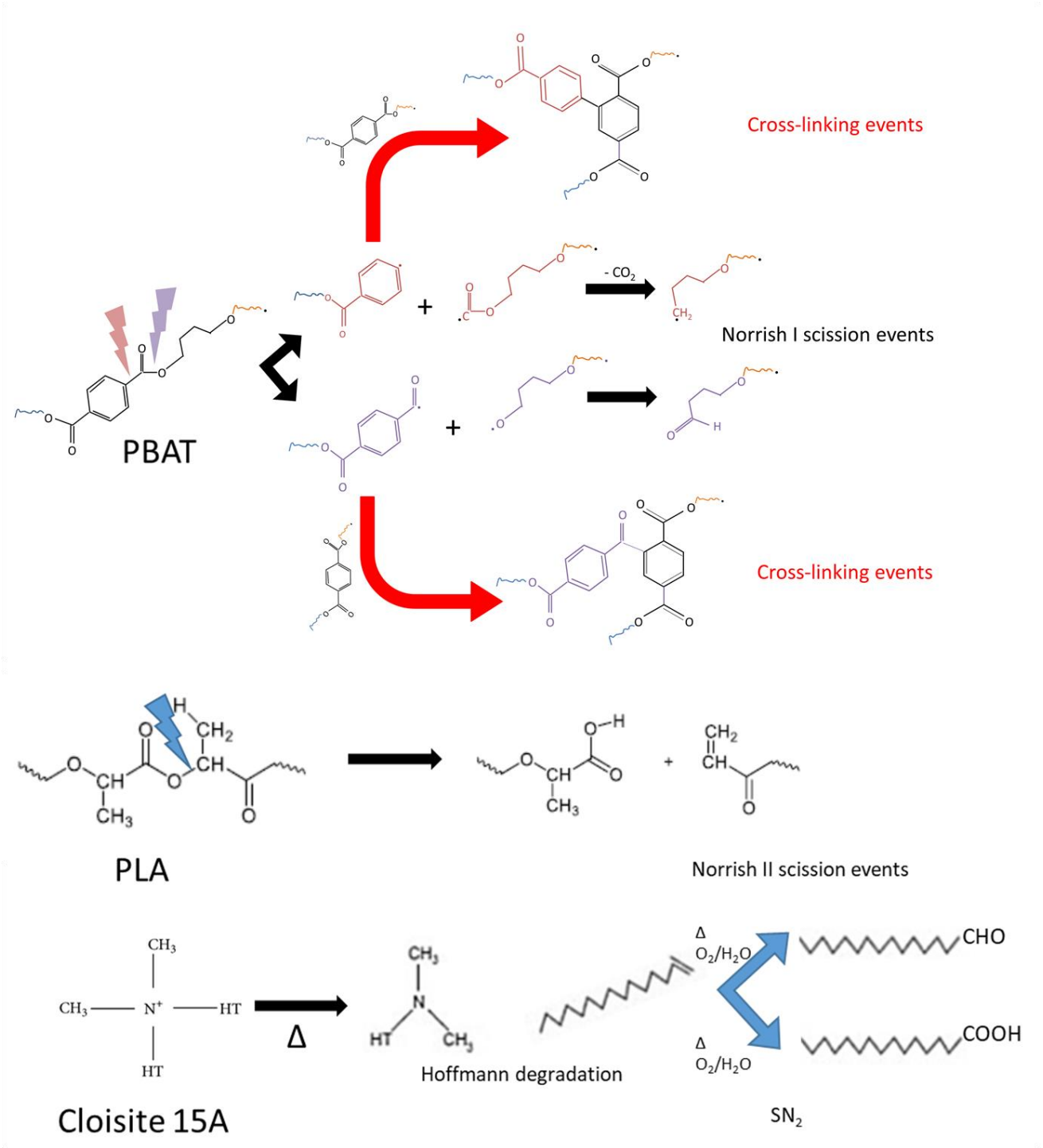

Figure 10. Possible photochemical degradation mechanisms of PBAT, PLA and Cloisite 15A.

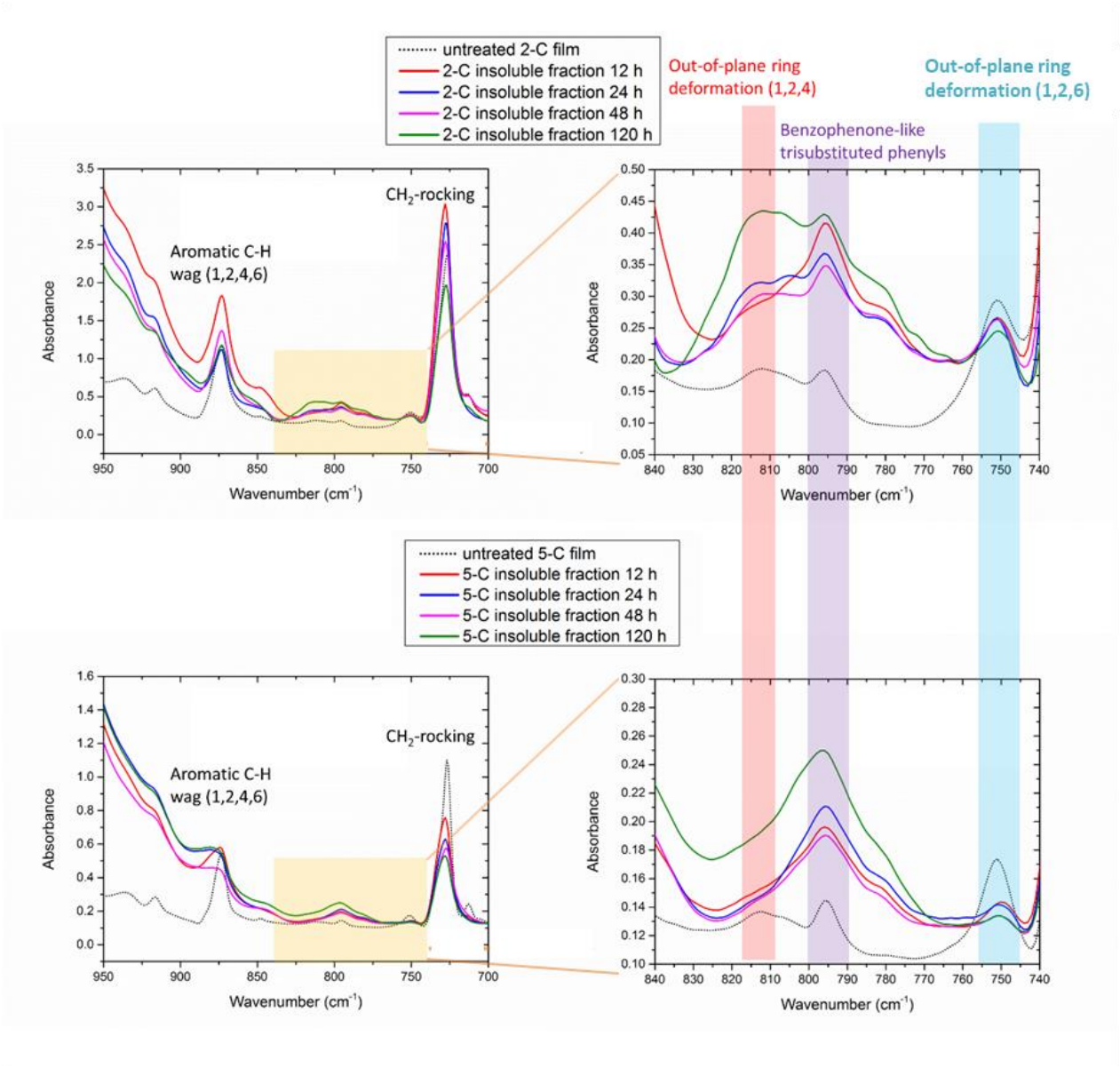

Figure 11. ATR/FTIR spectra in the spectral range 950-700 cm^{-1} of 2-C (top) and 5-C (bottom) crosslinked networks together with those of corresponding untreated films. Inset: close-up of range: 840-740 cm^{-1}.

Aromatic rings of PBAT products, evolving into phenyl or acyl radicals, play a crucial role and the presence of trisubstituted benzenes or benzophenone-like structures can be taken as an indicator to qualitatively assess these events [24–26]. A useful strategy to assess the structural changes occurring in the aromatic part of such systems is performing FTIR analysis onto insoluble fractions of 2-C and 5-C. **Figure 11** provides ATR spectra of 2-C and 5-C insoluble dried gels in the wavenumber range: 950-700 cm^{-1} together with those of untreated 2-C and 5-C films as reference

plots. In fact, the eventual occurrence of bands in this spectral region relate to various 1,2,4-trisubstituted benzenes (815 cm^{-1}), and benzophenones (at 795 cm^{-1}), which often are found to overlap depending on the distribution of molecular weights of the substituents and, especially, on the chemical nature of radicals that recombine each other [24–26,29].

The analysis of such spectra put into evidence that the insoluble fractions of both samples, at the various irradiation times, display a progressive decrease of the peak at 729 cm^{-1}, assigned to C-H rocking of butylene segments of PBAT, accompanied by the insurgence of a variegated band in the wavenumber range: 840-770 cm^{-1}. In this latter regard, at low clay contents (2-C), the modes centred at 815 cm^{-1} and 795 cm^{-1} displayed comparable intensity, thus indicating the presence of both 1,2,4-trisubstituted benzenes and trisubstituted benzophenones, while the latter ones were found prominent in 5-C crosslinked networks. It can be hypothesized that the organoclay affects the photochemical pathways, likely promoting the formation of acyl radicals that evolve into benzophenone-like structures, which are responsible for a more rapid and intense propagation of photochemical reaction, thus enabling the network formation even in the inner core of the films, and that this feature is more remarkable as the clay content increases.

As stated above, in long-term UV-exposure the degradation products of PBAT and PLA may recombine each other to yield branching or crosslinking reactions. To get rid of the eventual presence of PLA segments in crosslinked networks, FTIR/ATR spectra of dried gels in the carbonyl region were analysed by multi-peak fitting and thus compared to those of untreated corresponding films. In fact, the shoulder located at ca. 1750 cm^{-1} was the most visible mode associated to PLA, due to its low content (4 wt.%) in Ecovio formulation. Nevertheless, during photolysis of the samples, the intensity of such mode proved to dramatically increase, until reaching intensity comparable with those of C=O signals of PBAT (see again Fig. 9b).

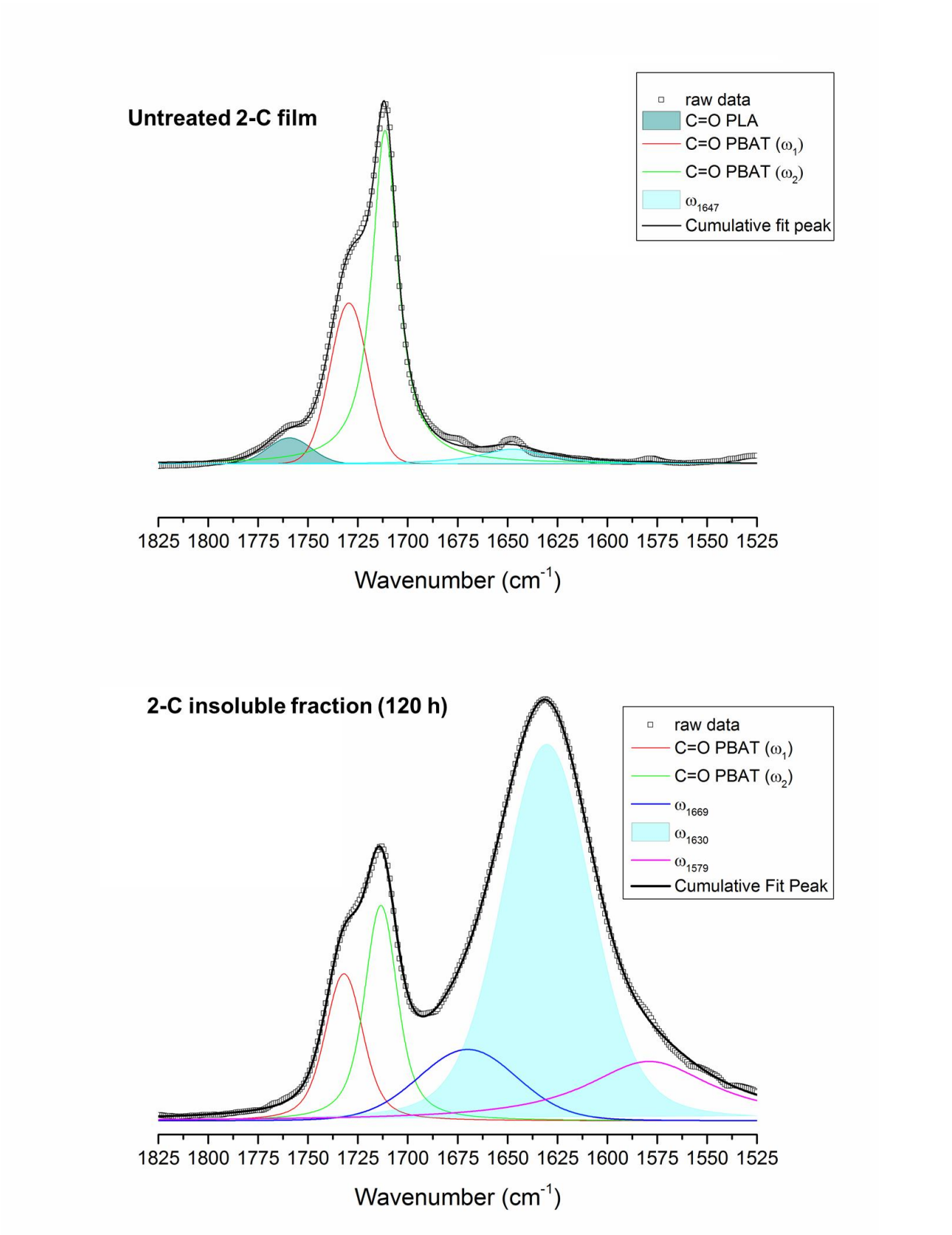

Figure 12. Deconvoluted carbonyl area for untreated 2-C film (top) and insoluble fraction extracted from 2-C irradiated for 120 h (bottom).

A comparison between crosslinked networks (after 120 h UV-exposure) and corresponding untreated films of 2-C sample is provided in **Figure 12**. The results demonstrate that no signals of PLA carbonyls could be detected in the insoluble fraction, suggesting that only PBAT is involved in crosslinking events. Moreover, the crosslinked network shows remarkable modes located at 1669, 1630 and 1579 cm^{-1}, likely attributable to the carbonyls of various low molecular weight aromatic esters [30].

4. Conclusions

Integration of various analytic methods was employed to assess macroscopic and structural transformations occurring during the photochemical weathering of bionanocomposites containing PBAT, PLA and organoclay. In particular, the pro-degradant role of nanofiller was unambiguously demonstrated: the higher the clay content, the higher the kinetics and the extent of both scission and crosslinking photochemical reactions, with relevant repercussions on mechanical and rheological properties of irradiated films.

Moreover, the isolation of insoluble fractions of nanocomposites, consisting of free-standing, porous structures, displaying an unprecedented thickness as high as 100 μm, allowed determining that the organoclay can increase the propagation depth of photochemical crosslinking by 10 times.

Ultimately, although the crosslinking mechanisms herein observed seem to be similar to those reported by other studies conducted on photochemical aging of PBAT and PBAT/PLA blends, the degradation extent of nanocomposites provides strong evidence for the pro-degradant effect of organoclay that accelerated the kinetics of chain cleavage and crosslinking events, maybe owing to the catalytic effect exerted by iron ions and decomposition products of alkylammonium salts. The crosslinked, insoluble networks formed due to UV-exposure revealed strong aromaticity and high porosity, with pore architecture and chemical structure strongly dependent on clay content. It could be hypothesized that the nanoclay, especially at high loadings, might have promoted the formation

of benzophenone-like moieties, thus increasing not only the kinetics but even the propagation depth of photochemical crosslinking.

The findings of this work, beyond the in-depth understanding of photochemical aging of PBAT/PLA blends in the presence of an organoclay, may represent a crucial step for the future development of porous structures from bioplastic wastes, otherwise problematic. In fact, photochemical weathering is well-known to dramatically reduce the biodegradability of PBAT-based materials [24] and the possibility to reuse them to fabricate high-added value materials may partially mitigate their overall environmental impact.

Acknowledgements

This work belongs to the PON project "Development and Application of Innovative Materials and Processes for the Diagnosis and Restoration of Cultural Heritage -DELIAS" (PON03PE_00214 2-DELIAS), funded by the MIUR.

Bibliography

[1] V. Nagarajan, A.K. Mohanty, M. Misra, Perspective on Polylactic Acid (PLA) based Sustainable Materials for Durable Applications: Focus on Toughness and Heat Resistance, ACS Sustain. Chem. Eng. 4 (2016) 2899–2916. https://doi.org/10.1021/acssuschemeng.6b00321.

[2] R. Scaffaro, A. Maio, F. Sutera, E.F. Gulino, M. Morreale, Degradation and recycling of films based on biodegradable polymers: a short review, Polymers (Basel). 11 (2019) 651. https://doi.org/10.3390/polym11040651.

[3] R. Scaffaro, A. Maio, E.F. Gulino, G. Pitarresi, Lignocellulosic fillers and graphene nanoplatelets as hybrid reinforcement for polylactic acid: Effect on mechanical properties and degradability, Compos. Sci. Technol. 190 (2020).

https://doi.org/10.1016/j.compscitech.2020.108008.

[4] H.-M. Park, M. Misra, L.T. Drzal, A.K. Mohanty, “Green” Nanocomposites from Cellulose Acetate Bioplastic and Clay: Effect of Eco-Friendly Triethyl Citrate Plasticizer, Biomacromolecules. 5 (2004) 2281–2288. https://doi.org/10.1021/bm049690f.

[5] R. Scaffaro, A. Maio, F. Lopresti, Physical properties of green composites based on poly-lactic acid or Mater-Bi® filled with Posidonia Oceanica leaves, Compos. Part A Appl. Sci. Manuf. 112 (2018) 315–327. https://doi.org/https://doi.org/10.1016/j.compositesa.2018.06.024.

[6] R. Scaffaro, A. Maio, E.F. Gulino, B. Megna, Structure-property relationship of PLA-Opuntia Ficus Indica biocomposites, Compos. Part B Eng. 167 (2019). https://doi.org/10.1016/j.compositesb.2018.12.025.

[7] A. Maio, M. Gammino, E. Fortunato Gulino, B. Megna, P. Fara, R. Scaffaro, Rapid One-Step Fabrication of Graphene Oxide-Decorated Polycaprolactone Three-Dimensional Templates for Water Treatment, ACS Appl. Polym. Mater. 0 (2020). https://doi.org/10.1021/acsapm.0c00852.

[8] R. Scaffaro, A. Maio, Integrated ternary bionanocomposites with superior mechanical performance via the synergistic role of graphene and plasma treated carbon nanotubes, Compos. Part B Eng. 168 (2019). https://doi.org/10.1016/j.compositesb.2019.03.076.

[9] A.L.P.D.L. Freitas, L.R. Tonini Filho, P.S. Calvão, A.M.C.D. Souza, Effect of montmorillonite and chain extender on rheological, morphological and biodegradation behavior of PLA/PBAT blends, Polym. Test. 62 (2017) 189–195. https://doi.org/10.1016/j.polymertesting.2017.06.030.

[10] S.-J. Xiong, B. Pang, S.-J. Zhou, M.-K. Li, S. Yang, Y.-Y. Wang, Q. Shi, S.-F. Wang, T.-Q.

Yuan, R.-C. Sun, Economically Competitive Biodegradable PBAT/Lignin Composites: Effect of Lignin Methylation and Compatibilizer, ACS Sustain. Chem. Eng. 8 (2020) 5338–5346. https://doi.org/10.1021/acssuschemeng.0c00789.

[11] R. Ghafari, R. Scaffaro, A. Maio, E.F. Gulino, G. Lo Re, M. Jonoobi, Processing-structure-property relationships of electrospun PLA-PEO membranes reinforced with enzymatic cellulose nanofibers, Polym. Test. 81 (2020). https://doi.org/10.1016/j.polymertesting.2019.106182.

[12] J. Trifol, D. Plackett, C. Sillard, P. Szabo, J. Bras, A.E. Daugaard, Hybrid poly(lactic acid)/nanocellulose/nanoclay composites with synergistically enhanced barrier properties and improved thermomechanical resistance, Polym. Int. (2016). https://doi.org/10.1002/pi.5154.

[13] O. Gordobil, I. Egüés, R. Llano-Ponte, J. Labidi, Physicochemical properties of PLA lignin blends, Polym. Degrad. Stab. 108 (2014) 330–338. https://doi.org/10.1016/j.polymdegradstab.2014.01.002.

[14] R. Scaffaro, A. Maio, E. Gulino, M. Morreale, F. Mantia, The effects of nanoclay on the mechanical properties, carvacrol release and degradation of a pla/pbat blend, Materials (Basel). 13 (2020). https://doi.org/10.3390/ma13040983.

[15] K. Sirisinha, W. Somboon, Melt characteristics, mechanical, and thermal properties of blown film from modified blends of poly(butylene adipate-co-terephthalate) and poly(lactide), J. Appl. Polym. Sci. 124 (2012) 4986–4992. https://doi.org/10.1002/app.35604.

[16] A. Iuliano, M. Nowacka, K. Rybak, M. Rzepna, The effects of electron beam radiation on material properties and degradation of commercial PBAT/PLA blend, J. Appl. Polym. Sci. 137 (2020). https://doi.org/10.1002/app.48462.

[17] M.C. Mistretta, F.P.L. Mantia, V. Titone, L. Botta, M. Pedeferri, M. Morreale, Effect of

ultraviolet and moisture action on biodegradable polymers and their blend, J. Appl. Biomater. Funct. Mater. 18 (2020) 1–8. https://doi.org/10.1177/2280800020926653.

[18] R. Scaffaro, A. Maio, Enhancing the mechanical performance of polymer based nanocomposites by plasma-modification of nanoparticles, Polym. Test. 31 (2012) 889–894. https://doi.org/10.1016/j.polymertesting.2012.06.006.

[19] R. Scaffaro, M.C. Mistretta, F.P. La Mantia, Compatibilized polyamide 6/polyethylene blend-clay nanocomposites: Effect of the degradation and stabilization of the clay modifier, Polym. Degrad. Stab. 93 (2008) 1267–1274. https://doi.org/10.1016/j.polymdegradstab.2008.04.008.

[20] R. Scaffaro, A. Maio, F.E. Gulino, C. Di Salvo, A. Arcarisi, Bilayer biodegradable films prepared by co-extrusion film blowing: Mechanical performance, release kinetics of an antimicrobial agent and hydrolytic degradation, Compos. Part A Appl. Sci. Manuf. 132 (2020). https://doi.org/10.1016/j.compositesa.2020.105836.

[21] H.R. Dennis, D.L. Hunter, D. Chang, S. Kim, J.L. White, J.W. Cho, D.R. Paul, Effect of melt processing conditions on the extent of exfoliation in organoclay-based nanocomposites, Polymer (Guildf). 42 (2001) 9513–9522. https://doi.org/10.1016/S0032-3861(01)00473-6.

[22] R. Scaffaro, A. Maio, G. Lo Re, A. Parisi, A. Busacca, Advanced piezoresistive sensor achieved by amphiphilic nanointerfaces of graphene oxide and biodegradable polymer blends, Compos. Sci. Technol. 156 (2018) 166–176. https://doi.org/https://doi.org/10.1016/j.compscitech.2018.01.008.

[23] R. Scaffaro, A. Maio, Influence of oxidation level of graphene oxide on the mechanical performance and photo-oxidation resistance of a polyamide 6, Polymers (Basel). 11 (2019). https://doi.org/10.3390/polym11050857.

[24] G.X. De Hoe, M.T. Zumstein, G.J. Getzinger, I. Rüegsegger, H.-P.E. Kohler, M.A. Maurer-Jones, M. Sander, M.A. Hillmyer, K. McNeill, Photochemical Transformation of Poly(butylene adipate- co-terephthalate) and Its Effects on Enzymatic Hydrolyzability, Environ. Sci. Technol. 53 (2019) 2472–2481. https://doi.org/10.1021/acs.est.8b06458.

[25] T. Kijchavengkul, R. Auras, M. Rubino, Measuring gel content of aromatic polyesters using FTIR spectrophotometry and DSC, Polym. Test. 27 (2008) 55–60. https://doi.org/10.1016/j.polymertesting.2007.08.007.

[26] M.A. Maurer-Jones, E.M. Monzo, Quantifying Photochemical Transformations of Poly(butylene adipate-co-terephthalate) Films, ACS Appl. Polym. Mater. (2021). https://doi.org/10.1021/acsapm.0c01283.

[27] T.M.D. Fernandes, M.C.A.M. Leite, A.M.F. de Sousa, C.R.G. Furtado, V.A. Escócio, A.L.N. da Silva, Improvement in toughness of polylactide/poly(butylene adipate-co-terephthalate) blend by adding nitrile rubber, Polym. Bull. 74 (2017) 1713–1726. https://doi.org/10.1007/s00289-016-1798-9.

[28] S. Kakuta, T. Okayama, M. Kato, A. Oda, T. Abe, Clarification of photocatalysis induced by iron ion species naturally contained in a clay compound, Catal. Sci. Technol. 1 (2011) 1671–1676. https://doi.org/10.1039/c1cy00286d.

[29] H. Jiang, J. Wang, S. Wu, Z. Yuan, Z. Hu, R. Wu, Q. Liu, The pyrolysis mechanism of phenol formaldehyde resin, Polym. Degrad. Stab. 97 (2012) 1527–1533. https://doi.org/10.1016/j.polymdegradstab.2012.04.016.

[30] J.-M. Wang, H. Wang, E.-C. Chen, Y.-J. Chen, T.-M. Wu, Enhanced photodegradation stability in poly(Butylene adipate-co-terephthalate) composites using organically modified layered zinc phenylphosphonate, Polymers (Basel). 12 (2020) 1–12. https://doi.org/10.3390/polym12091968.

Supporting information

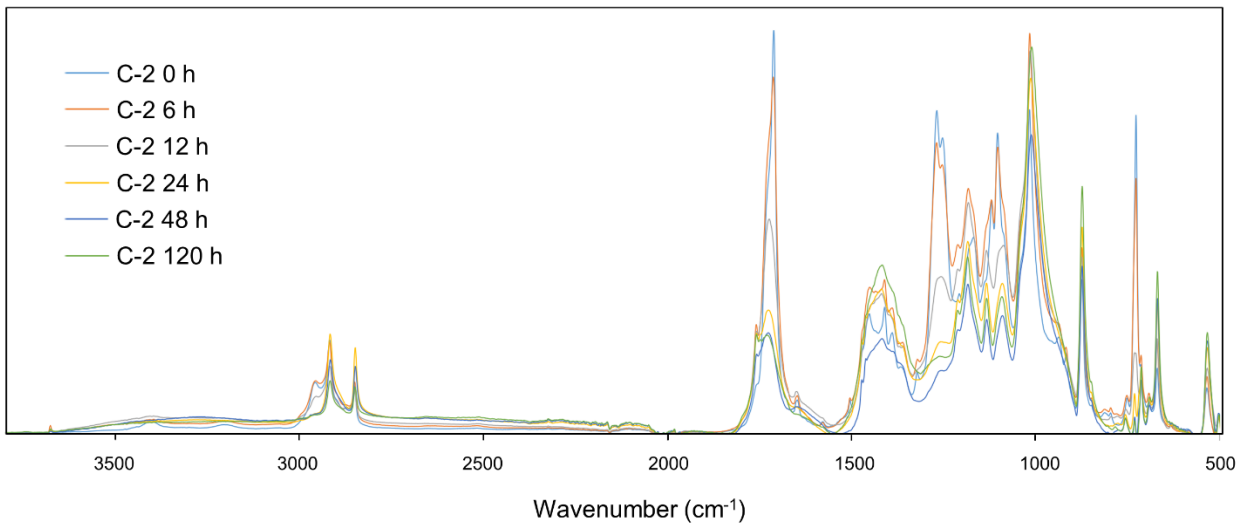

Figure S1. FTIR/ATR spectra of 2-C

Declaration of interests

☒ The authors declare that they have no known competing financial interests or personal relationships that could have appeared to influence the work reported in this paper.

☐The authors declare the following financial interests/personal relationships which may be considered as potential competing interests: